

Florida State University Libraries

2019

A Search for the Production of Axion-Like Particles Decaying to Photons at $\sqrt{s} = 13$ TeV

Adam Albert Kobert



The Florida State University
College of Arts and Sciences

A SEARCH FOR THE PRODUCTION OF LOW MASS AXION-LIKE
PARTICLES DECAYING TO PHOTONS AT $\sqrt{s} = 13$ TeV

By

ADAM KOBERT

A Thesis submitted to the Department of Physics in partial fulfillment of
the requirements for graduation with Honors in the Major


Bachelors of Science in Physics
Spring, 2019

The members of the Defense Committee approve the thesis of Adam
Kobert defended on April 16, 2019

A handwritten signature in black ink, appearing to read 'Andrew Askew', written over a horizontal line.

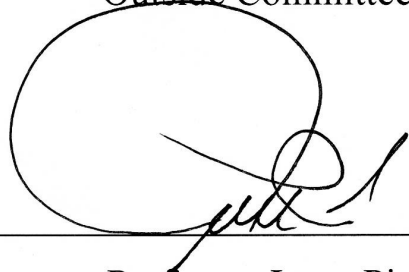
Associate Professor Andrew Askew

Thesis Director

A handwritten signature in black ink, appearing to read 'David Gaitros', written over a horizontal line.

Senior Teaching Faculty David Gaitros

Outside Committee Member

A handwritten signature in black ink, appearing to read 'Jorge Piekarewicz', written over a horizontal line. The signature is stylized with a large loop.

Professor Jorge Piekarewicz

Committee Member

Abstract

This thesis presents a search for axion-like-particles (ALPs) decaying to two photons in the low mass region (5 to 85 GeV) using data collected by the CMS experiment in 2018 at $\sqrt{s} = 13$ TeV in 2018. The unique aspect of this thesis is the requirement of Initial State Radiation (ISR), which is a photon or jet emitted by one of the incident quarks in the collision. Two final states are selected, the first had an ISR photon for a three photon final state based on a 54.67 fb^{-1} luminosity sample. The second had an ISR jet for a two photon plus jet final state based on a 59.96 fb^{-1} luminosity sample. No evidence for the production of ALPs was observed.

Contents

Contents	4
List of Figures	5
1 Intro and Motivation	6
2 Detector Information	7
2.1 Coordinate System	7
2.2 Electromagnetic Calorimeter	10
2.2.1 Trigger	10
2.2.2 Clustering	10
2.2.3 Pixel Match	11
2.2.4 Shower Shape	11
2.2.5 H/E	11
3 Selection and Background	12
3.1 Case 1	12
3.1.1 Selection	12
3.1.2 Plots	14
3.2 Case 2	16
3.2.1 Selection	17
3.2.2 Plots	18
4 Analysis	21
4.1 Background Fit	21
4.2 Signal Fit	25
4.3 Hypothesis Testing	29
5 Conclusions	36
References	37

List of Figures

1	Diagram of Basic Collision Topology	6
2	Cross Section of the CMS Detector	7
3	Phi Diagram	8
4	Theta Diagram	8
5	ΔR Diagram	9
6	CMS Detector Sections	10
7	Electromagnetic Shower	10
8	Crystal Clustering	11
9	Case 1 Final State	12
10	Case 1 Event Display	13
11	Case 1 Invariant Mass Histogram	14
12	Case 1 ΔR Particle 1	15
13	Case 1 ΔR Particle 2	15
14	Case 1 Invariant Mass Histogram (Control Sample)	16
15	Case 2 Final State	17
16	Case 2 Event Display	18
17	Case 2 Invariant Mass Histogram	19
18	Case 2 ΔR	19
19	Case 2 Invariant Mass Histogram (Control Sample)	20
20	Functional Fit of Case 1 Control Sample	21
21	Functional Fit of Case 1 Control Sample Log Scale	22
22	Case 1 Fit Residuals	22
23	Functional Fit of Case 2 Control Sample	23
24	Functional Fit of Case 2 Control Sample Log Scale	24
25	Case 2 Fit Residuals	24
26	Case 1 Candidate Sample Fit	25
27	Case 1 Candidate Sample Gaussian Fit	26
28	Case 2 Candidate Sample Fit	27
29	Case 2 Candidate Sample Gaussian Fit	27
30	Signal Strength as a Function of Gaussian Mean for Case 1 Candidate Sample	28
31	Signal Strength as a Function of Gaussian Mean for Case 2 Candidate Sample	29
32	Case 1 Pseudo Data Fits Amplitude Parameter Plot	30
33	Case 1 Pseudo Data Fits Exponential Parameter Plot	30
34	Case 1 Pseudo Data Fits Exponential2 Parameter Plot	31
35	Case 1 Pseudo Data Fits Probability Plot	31
36	Case 1 Pseudo Data Fits Amplitude Parameter Plot	32
37	Case 1 Pseudo Data Fits Exponential2 Parameter Plot	32
38	Case 1 Pseudo Data Fits Probability Plot	33
39	Case 1 Pseudo Data Maximum Signal Strengths	34
40	Case 2 Pseudo Data Maximum Signal Strengths	34

1 Intro and Motivation

The Standard Model (SM) of particle physics describes all known types of particles and forces (aside from gravity). However, issues with the theory still persist, with one of the major lingering problems being the Strong CP Problem. Charge-parity (CP) symmetry states that when a particle is replaced with its antiparticle, and its spatial coordinates are inverted the laws of physics for said particle would be unchanged. Violation of this symmetry was observed in 1964 with the decay of neutral kaons. However violation of CP in strong interactions has been detected very rarely, meaning that the parameter for CP violation in strong interactions must be very small [1]. One recent example of this rare strong CP violation was with the D^0 meson decaying to kaons and pions at the LHCb collaboration at CERN. This raises the question that if CP is violated extremely rarely, why is there so much more matter than antimatter? The axion provides a solution to this problem, where the production of axions through gluon-gluon (strong) interactions would violate CP symmetry at relatively low energies[2].

The model used to search for these low mass axion-Like-Particles (ALPs) is motivated by a paper published in 2018. In this paper the model for an ALP with an invariant mass between 10 and 65 GeV decaying to a pair of photons is put forward (a possible decay to a pair of jets is also considered)[3].

The focus of this thesis was a search for statistically significant evidence of the production of axion-like-particles at the Large-Hadron Collider (LHC). To do so, a search for a diphoton resonance signature was used. A diphoton resonance search revolves around using pairs of photons to reconstruct the invariant mass of the particle that decayed into them. Previous papers which use searches of this type note that this method allows for the mass of the decaying object to be reconstructed to high precision, even with large backgrounds[5]. The search being performed looked for a narrow excess against the background, the presence of which would be evidence for the production of ALPs of that mass.

The unique aspect of this thesis was the requirement of the presence of Initial State Radiation (ISR). ISR is any kind of particle emitted by one of the incident particles in the model, in the cases being considered this ISR can be a photon or a gluon. Requiring ISR as a criteria in selecting events has two benefits. First, recoiling off the ISR will boost the photons that will be detected to a higher energy making them easier to detect. Second, when triggering on the ISR, decay photons can be at a low energy without and not have to meet trigger requirements (which will be explained in Section 2.2.1). The resulting model with the ISR requirement can be seen in Figure 1.

The data for this search comes from the 2018 data of the Compact Muon Solenoid (CMS). Two final states are selected, the first had an ISR photon for a three photon final state based on a 54.67 fb^{-1} luminosity sample. The second had an ISR jet for a two photon plus jet final state based on a 59.96 fb^{-1} luminosity sample.

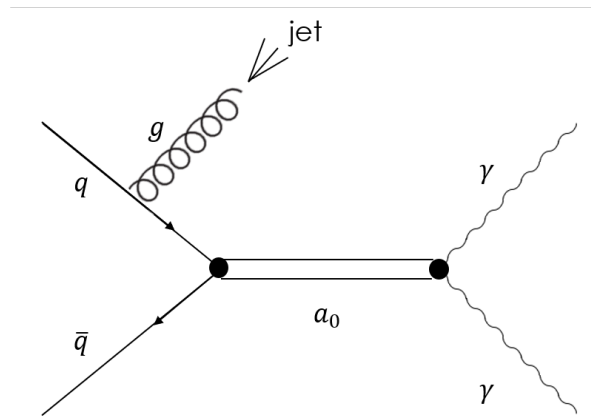


Figure 1: In this diagram one of the incident quarks emits a gluon which fragments into a jet as ISR, an ALP is created, which subsequently decays into two photons

2 Detector Information

The data used in this analysis comes from the 2018 Compact Muon Solenoid (CMS) with $\sqrt{s} = 13$ TeV at the LHC. The CMS detector consists of many layers as seen in Figure 2. These layers are the silicon tracker, the electromagnetic calorimeter (ECAL), the hadron calorimeter (HCAL), the superconducting magnet, and the muon detector chambers. For the purposes of this thesis the ECAL will provide most of the relevant information.

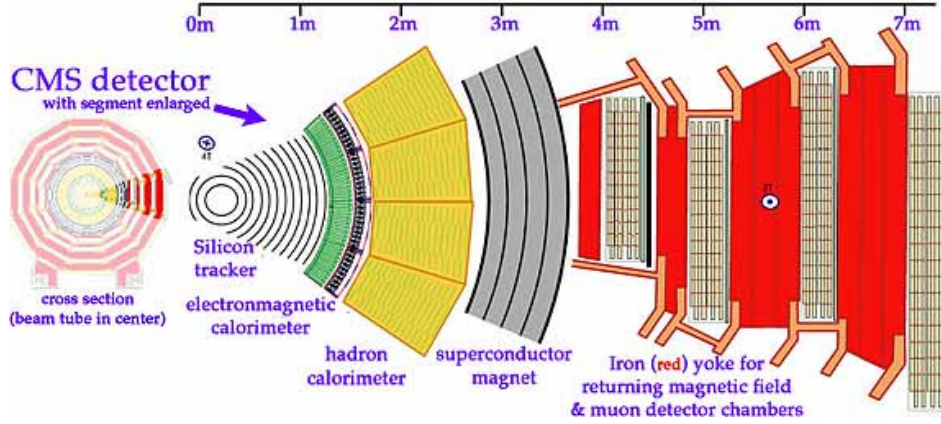


Figure 2: Cross section of the CMS detector. Layers from inside to outside are the silicon tracker, the electromagnetic calorimeter (ECAL), the hadron calorimeter (HCAL), the superconductor magnet, and the muon chambers[6].

2.1 Coordinate System

The coordinate system used in the CMS detector consists of three values η , ϕ , and ρ . ϕ is the azimuthal angle, with $\phi = 0$ always pointing toward the center of the collider, this is shown in Figure 3. η is slightly more complicated, using Equation 1 η can be found from θ (the polar angle) which is the angle from the beam line (+z axis). ρ is radial distance from the center of the detector.

$$\eta = -\ln\left(\tan\left(\frac{\theta}{2}\right)\right) \quad (1)$$

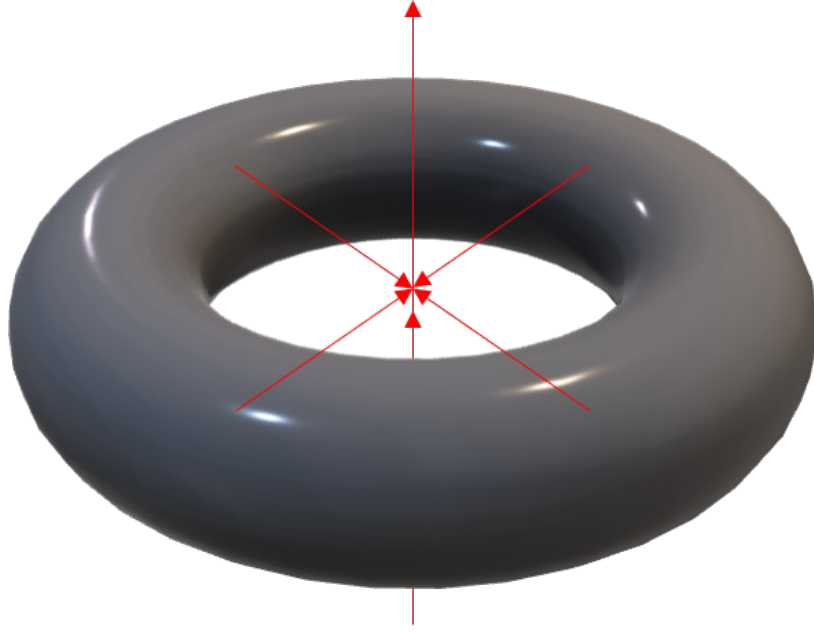


Figure 3: This figure shows a zoomed out depiction of the Collider ring. $\phi = 0$ always points toward the center of the Collider.

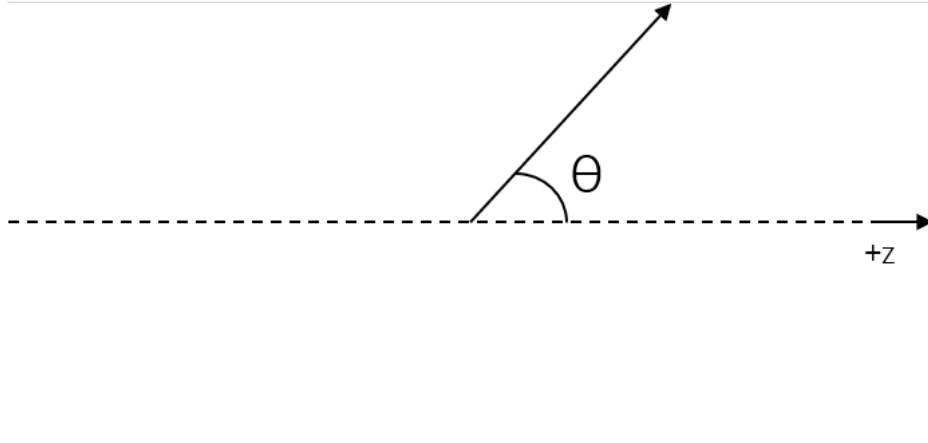


Figure 4: The counterclockwise proton beam line is in the $+z$ direction, the angle from the z direction is θ .

This coordinate system is important when calculating various values from the data. These values are:

1. Transverse energy found in Equation 2 which is energy transverse to the beam line. This is important because in the laboratory frame, no momentum is transverse to the beam line, all momentum transverse to the beam line was created from the collision.
2. ΔR is the distance between two trajectories in the η - ϕ phase space, defined in Equation 3. This distance is shown in Figure 5.

3. Invariant mass of the particle from a two-particle decay is found in Equation 4. For massless particles like photons the m_1 and m_2 will be zero.

$$E_T = E \sin \theta \quad (2)$$

$$\Delta R = \sqrt{\Delta \eta^2 + \Delta \phi^2} \quad (3)$$

$$m_0 = \sqrt{m_1^2 + m_2^2 + 2(E_1 * E_2 - \vec{p}_1 \cdot \vec{p}_2)} \quad (4)$$

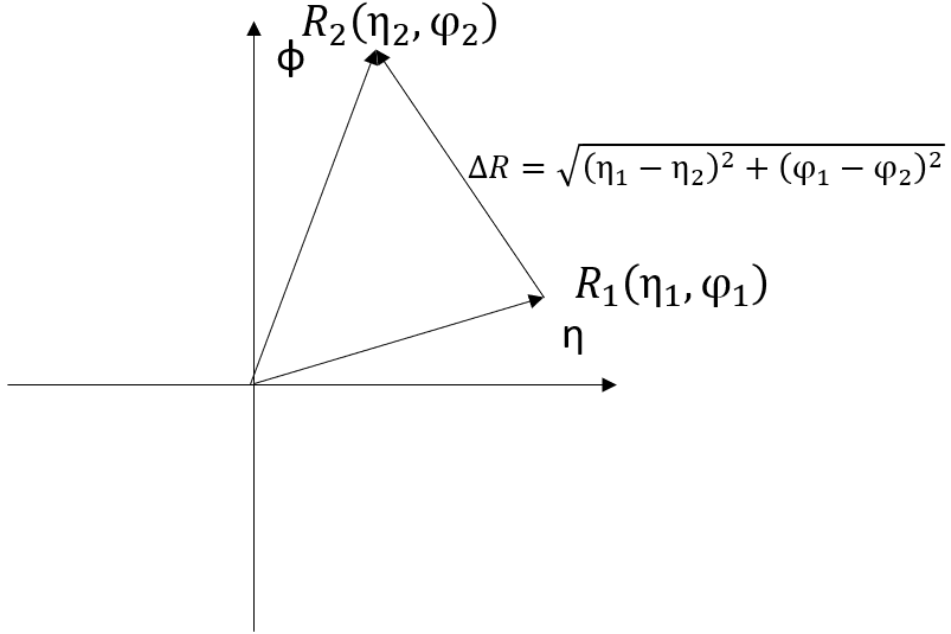


Figure 5: ΔR , the distance between two locations in the η - ϕ phase space

This coordinate system also helps define the two distinct sections of the CMS detector ECAL. The barrel is defined where $|\eta| < 1.44$, the end cap is defined where $1.55 < |\eta| < 2.5$. This can be seen in Figure 6 where the forward calorimeter is the end cap and the main section is the barrel.

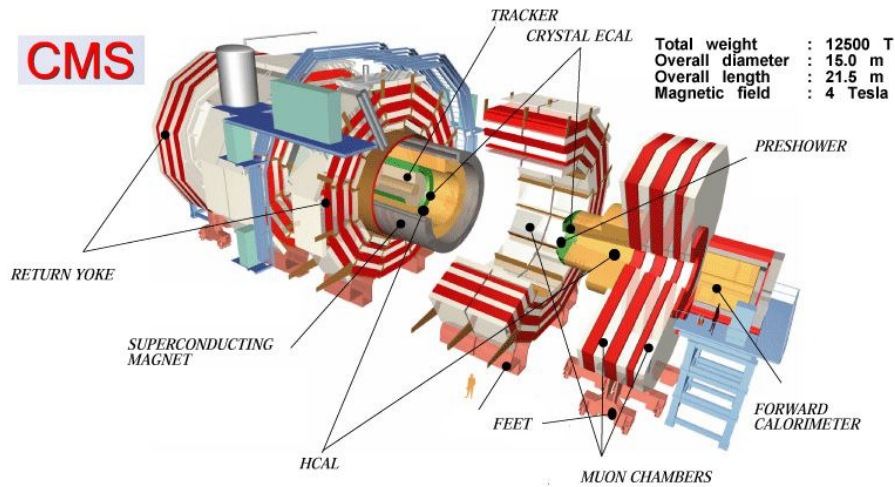


Figure 6: Split up view of the different sections of the CMS detector. [7]

2.2 Electromagnetic Calorimeter

The ECAL consists mainly of a large lattice of lead tungstate crystals which scintillate when electrons and photons pass through them. The amount of light produced will be proportional to the particle's energy. When a photon or electron passes through one of the lead tungstate crystals, an electromagnetic shower is created like the one shown in Figure 7. At the end of each crystal a photo-detector is attached to determine the amount of light (corresponding to the magnitude of energy deposited) in each crystal.

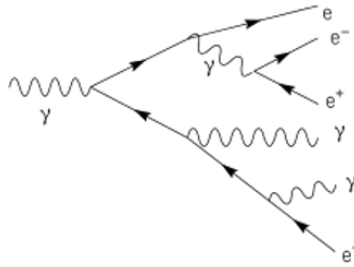


Figure 7: Electromagnetic shower, photon converts into electron-positron pair, which emit Bremsstrahlung photons, which split, etc. [8]

2.2.1 Trigger

Due to the sheer scale of the data that the LHC produces, low level requirements are put in place to limit the amount of data that is actually recorded. The requirements vary with time and by experiment, but in the case of this project, the trigger will require the presence of photons with specific qualities.

In the first case examined the trigger requires an ISR photon with a Transverse Energy above 110 GeV, with additional requirements for the shower shape (Section 2.2.4), H/E (Section 2.2.5), and isolation (Section 2.2.2). In the second case examined the trigger requires one of the decay photons to have a transverse energy above 200 GeV and no other requirements.

2.2.2 Clustering

The deposited energy in each crystal by itself is insufficient to reconstruct the details of each event. Crystals with energy deposited into them are grouped into clusters as seen in Figure 8. The exact

distribution and magnitude of energy in each cluster gives information about the particle that created the cluster.

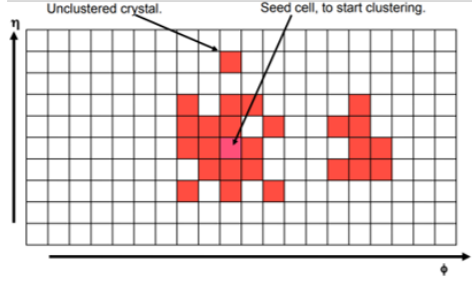


Figure 8: Energy contained within each crystal is clustered into distinct groups. [4]

Once clusters are formed the reconstruction algorithms will then try to group clusters in close proximity into superclusters. These superclusters become the photon candidates that are examined in this thesis.

Isolation requirements are also put in place so no jets are in the immediate vicinity, this helps ensure that none of the photon candidates are jets that have been reinterpreted as photons. The exact requirements are complex, but in essence, the ratio of energy from other sources (mostly hadrons produced from jets) to the transverse energy of the cluster must be below a certain threshold.

2.2.3 Pixel Match

When a charged particle passes through the silicon tracker, ionization energy is deposited in different layers of the tracker. If a triplet of deposits that define a helical trajectory is present a seed is created. If a seed trajectory can be extrapolated to the location of a cluster this is a pixel match. If a pixel match exists then it can be reasonably assumed that the particle which created the cluster was a charged particle (likely an electron). For this search, photons are the primary reconstruction target, so all reconstruction candidates were required not to have a pixel match.

2.2.4 Shower Shape

Due to the situation where photons being measured are in extreme proximity to each other, the usual method of requiring isolation of clusters will not work (Section 2.2.2), instead shower shape ($\sigma_{i\eta i\eta}$) requirements are put in place. The shower shape is the weighted energy distribution width within a cluster, calculated using Equation 5. The shower shape measurement varies based on its location and the type of particle which created it (i.e. jets tend to have a broader energy distribution than photons). By requiring the reconstructed photons to be within a certain shower shape, we can reasonably assume they are actually photons.[4]

$$\sigma_{i\eta i\eta}^2 = \frac{\sum_{5x5} w_i (\bar{\eta} - \eta_i)^2}{\sum_{5x5}} \quad (5)$$

$$w_i = \max(0, w_0 + \ln \frac{E_i}{E_{5x5}}) \quad (6)$$

$$w_0 = 4.7$$

2.2.5 H/E

H/E is the ratio between the energy in the HCAL tower located immediately behind the supercluster seed and the energy in the ECAL deposited in the supercluster. If this ratio is high, then it is likely that the energy in the cluster originated from a hadron and is not relevant to this search.

3 Selection and Background

With the final state seen in Figure 1 in mind, more specific topologies can be defined to select the candidate events for the production of ALPs. These topologies are defined by the objects required and their kinematics. By cutting events which deviate from these requirements, the remaining events are candidates for the production of ALPs. In this thesis, two cases were examined.

In the first case, the ISR is a photon which also functions as the trigger for the event. In the second case, the ISR is a gluon which fragments into a jet, while the trigger for the event is one of the decay photons.

3.1 Case 1

In this case, the ISR is a photon, while the ALP recoils in the opposite direction decaying into two photons; thereby forming a three photon final state. The trigger is the ISR photon with a minimum threshold of 110 GeV. Having the trigger be on the ISR allows the detected decay photons to be at a low energy and not have to meet trigger requirements. A diagram of the final state can be seen in Figure 9.

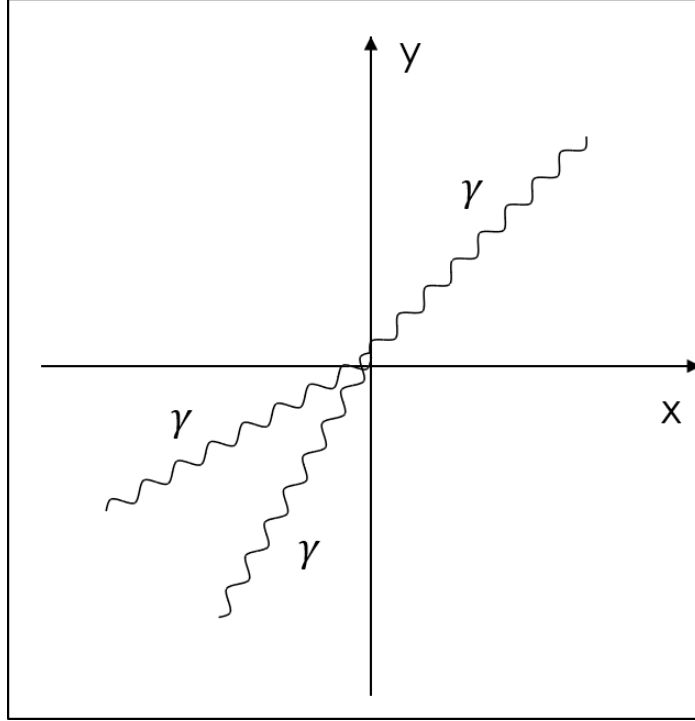


Figure 9: Case 1 final state. ISR photon goes in one direction, while the two decay photons recoil in the direct opposite direction

3.1.1 Selection

In order to properly select the events corresponding to the desired model, a series of selection cuts are required:

- The photon which acts as the trigger object must have E_T greater than 120 GeV and be located in the barrel,

- All photon candidates must have a pixel match of zero, indicating that this object is a photon, not an electron,
- All photon candidates must have above 15 GeV of transverse energy (E_T), this requirement helps eliminate events reconstructed from photons created by the passage of charged particles through the ECAL (bremsstrahlung radiation),
- In addition to the photon which acts as a trigger, at least two other photon candidates must be present,
- ΔR between all photon candidates and the trigger photon must be above 0.1, this means the trigger photon is kept separate from the photon candidates,
- Barrel photon candidates must have an H/E value less than 0.04596,
- End-cap photon candidates must have an H/E value less than 0.059,
- Barrel photon candidates $\sigma_{i\eta i\eta}$ must be less than 0.0106,
- End-cap photon candidates $\sigma_{i\eta i\eta}$ must be less than 0.0272,
- Barrel photon candidates must have an $|\eta|$ less than 1.44,
- Endcap photon candidates must have an $|\eta|$ between 1.55 and 2.5.

From the list of photon candidates for the barrel and endcap, the two highest transverse energy photon candidates from each are selected. Combinations of photons are considered, barrel-barrel, endcap-endcap, and barrel-endcap. If the ΔR between two non-trigger photons in a combination (presuming enough are present) is between 0.1 and 0.4, the invariant mass of the particle which decays into these photons will be calculated (along with other information).

After all the candidate events were selected, a few of the events with a high decay pair transverse energy were examined. The events with pairs of photons with high E_T were examined to ensure they corresponded to the specific event topology being selected. In Figure 10 an event display for one of these events is shown, and it corresponds to the topology being selected, with a pair of photons in close proximity recoiling off a high E_T photon.

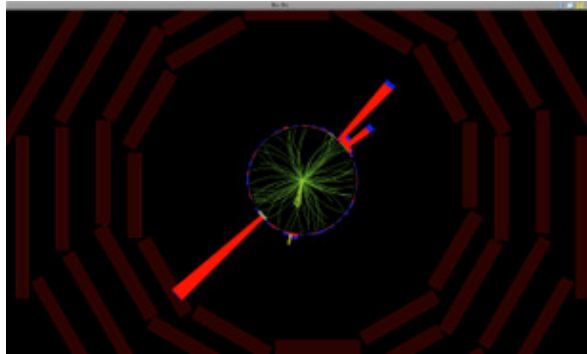


Figure 10: Event display of CMS detector in the $\rho - \phi$ perspective for interesting event. Large red bars are the photons, green lines are tracks, yellow bar is jet. It is clear to see that a pair of high E_T photons are recoiling off a single high E_T photon.

A second set of plots must be generated which exclude any possible signal. This set of plots will be used to generate a functional form for the background. To ensure that these plots consist of events which have identical criteria to the candidate events but without any possible ALPs being allowed in,

the $\sigma_{i\eta i\eta}$ (shower shape) requirements from earlier are reversed. In this distribution, at least one of the photons from the ALP decay must have a $\sigma_{i\eta i\eta}$ above a certain threshold (0.0106 in barrel, 0.0272 in end cap). Requiring the shower shape to fail for at least one of the photons in the pair will ensure that the event is not one of the possible candidates and solely consists of background noise.

3.1.2 Plots

After the invariant mass plots for each combination are generated, the plots are then combined as seen in Figure 11. This is known as the candidate sample.

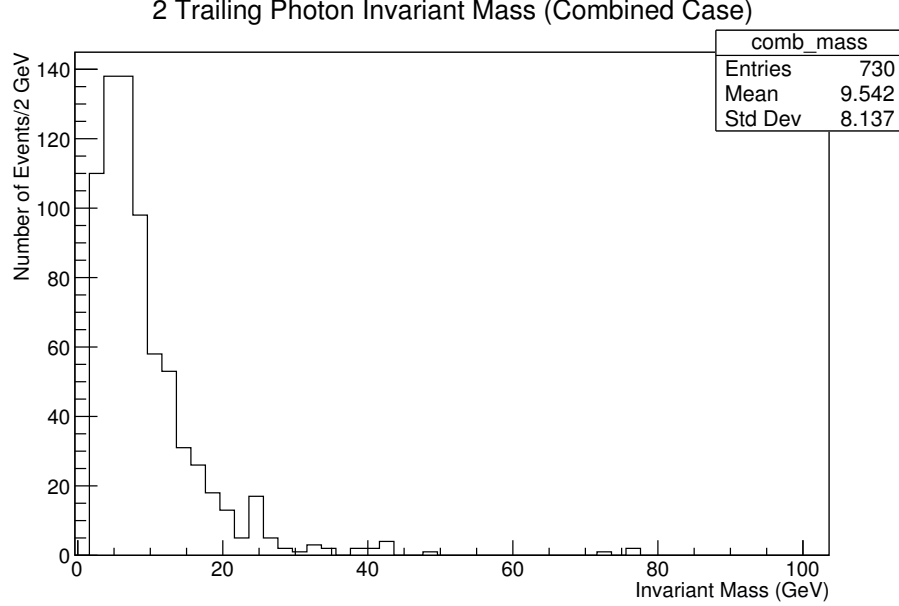


Figure 11: Case 1 Invariant Mass Histogram (Candidate Sample)

According to momentum conservation, the decay photons should recoil opposite of the trigger photon. In Figures 12 and 13, the direct recoiling of the decay photons from the trigger photon is shown with a $\Delta R \sim 3.5$ (directly opposite trajectories) is shown.

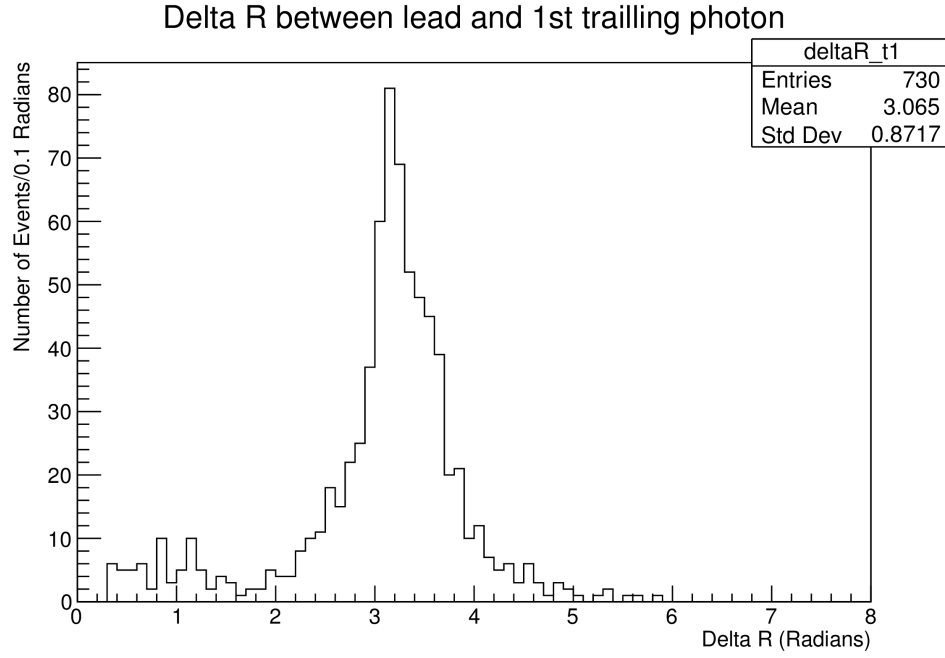


Figure 12: Case 1 ΔR between the trigger photon and the highest transverse energy decay photon

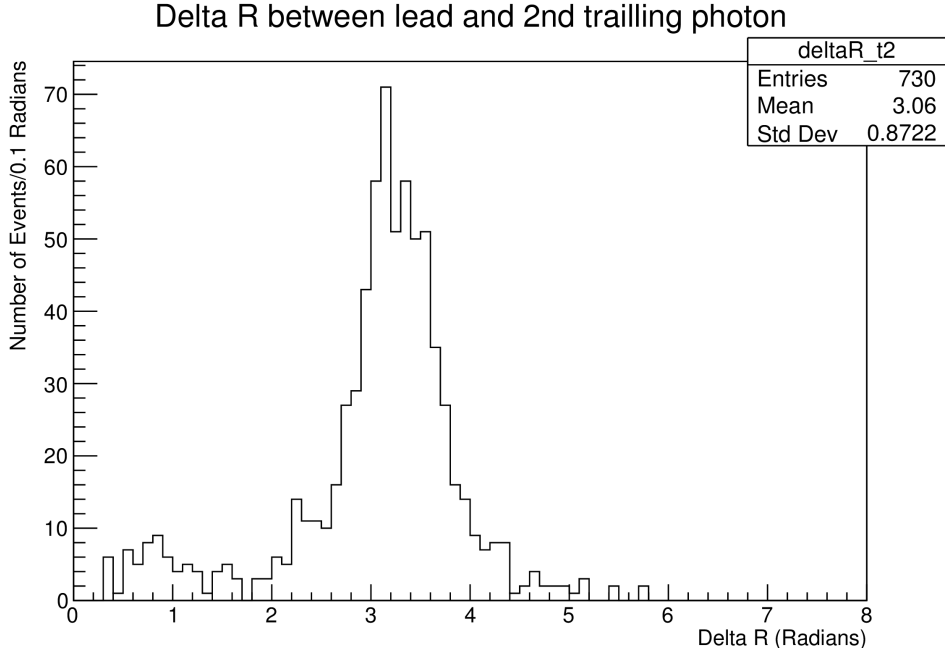


Figure 13: Case 1 ΔR between the trigger photon and the second highest transverse energy decay photon

With the background criteria specified earlier, the mass plot for the control sample is seen in Figure 14.

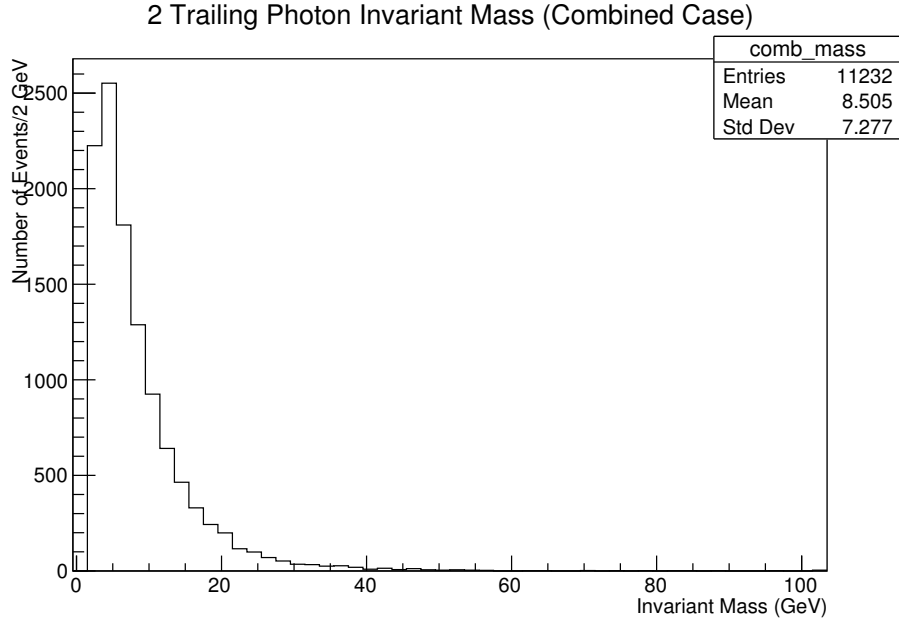


Figure 14: Case 1 Invariant Mass Histogram (control sample)

3.2 Case 2

In this case, the ISR is a gluon which fragments into a jet, while the ALP recoils in the opposite direction decaying to two photons; thereby forming a two photon and one jet final state. The trigger is highest energy decay photon with a minimum threshold of 200 GeV. A diagram of the final state can be seen in Figure 15.

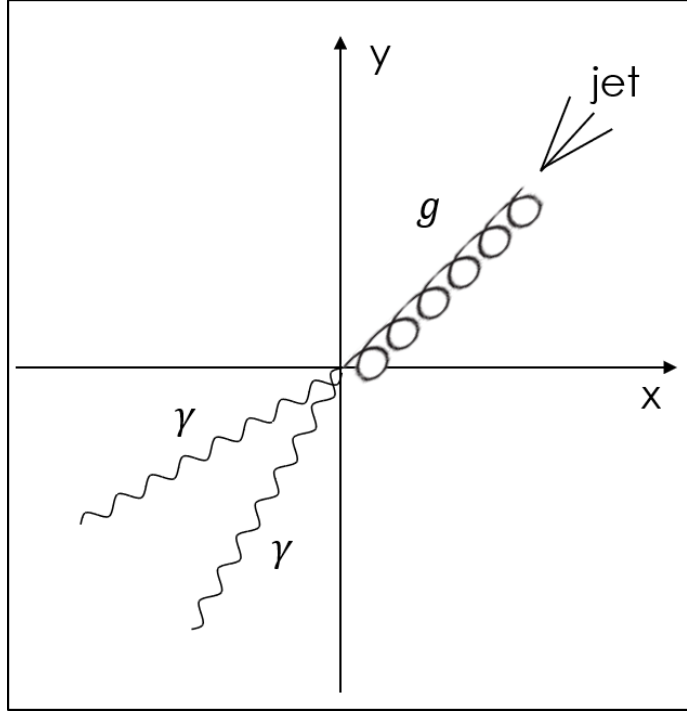


Figure 15: Case 2 final state. ISR jet goes in one direction, while the two decay photons recoil in the direct opposite direction

3.2.1 Selection

In order to properly select the events corresponding to the desired model, a series of selection cuts are required:

- The photon which acts as the trigger object must have E_T greater than 225 GeV,
- All photon candidates must have a pixel match of zero, indicating that this object is a photon, not an electron,
- All photon candidates must have at least 15 GeV of transverse energy (E_T), this requirement helps eliminate events reconstructed from photons created by the passage of charged particles through the ECAL (bremsstrahlung radiation),
- In addition to the photon which acts as a trigger, at least one other photon candidate must be present,
- Barrel photon candidates must have an H/E value less than 0.04596,
- End-cap photon candidates must have an H/E value less than 0.059,
- Barrel photon candidates $\sigma_{i\eta i\eta}$ must be less than 0.0106,
- End-cap photon candidates $\sigma_{i\eta i\eta}$ must be less than 0.0272,
- Barrel photon candidates must have an $|\eta|$ less than 1.44,
- End-cap photon candidates must have an $|\eta|$ between 1.55 and 2.5,
- The highest transverse energy photon of the barrel or end-cap must be the trigger photon,

- A jet with at least 100 GeV of transverse energy (E_T) must be present,
- The highest energy jet must have a photon fraction less than 0.9,
- The highest energy jet must have a ΔR greater than 0.4 from all considered photons.

From the list of photon candidates for the barrel and endcap, the two highest transverse energy photon candidates from each are selected. Combinations of photons are considered, barrel-barrel, end cap-endcap, barrel-endcap (trigger on barrel photon), endcap-barrel (trigger on end cap photon). If the ΔR between two photons in a combination (presuming enough are present) is between 0.1 and 0.4, the invariant mass of the particle which decays into these photons will be calculated (along with other information).

After all the candidate events were selected, a few of the events with a high decay pair transverse energy were examined. The events with pairs of photons with high E_T were examined to ensure they corresponded to the specific event topology being selected. In Figure 16 an event display for one of these events is shown, and it corresponds to the topology being selected, with a pair of photons in close proximity recoiling off a high E_T jet.

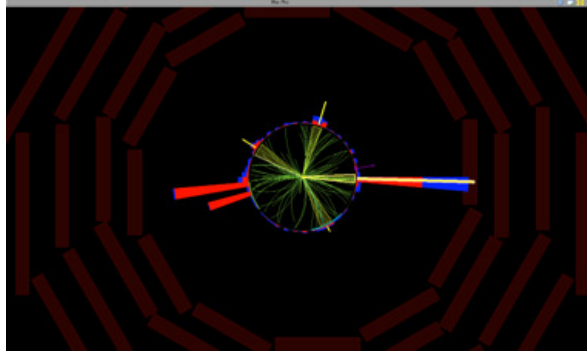


Figure 16: Event display of CMS detector in the $\rho - \phi$ perspective for interesting event. Large red bars are the photons, green lines are tracks, yellow bars are jets. It is clear to see that a pair of high E_T photons are recoiling off a single high E_T jet.

A second set of plots must be generated which exclude any possible signal. This set of plots will be used to generate a functional form for the background. To ensure that these plots consist of events which have identical criteria to the candidate events but without any possible ALPs being allowed in, the $\sigma_{i\eta i\eta}$ (shower shape) requirements from earlier are reversed. In this distribution, at least one of the photons from the ALP decay must have a $\sigma_{i\eta i\eta}$ above a certain threshold (0.0106 in barrel, 0.0272 in end cap). Requiring the shower shape to fail for at least one of the photons in the pair will ensure that the event is not one of the possible candidates and solely consists of background noise.

3.2.2 Plots

After the invariant mass plots for each combination are generated, the plots are then combined as seen in Figure 17. This is known as the candidate sample.

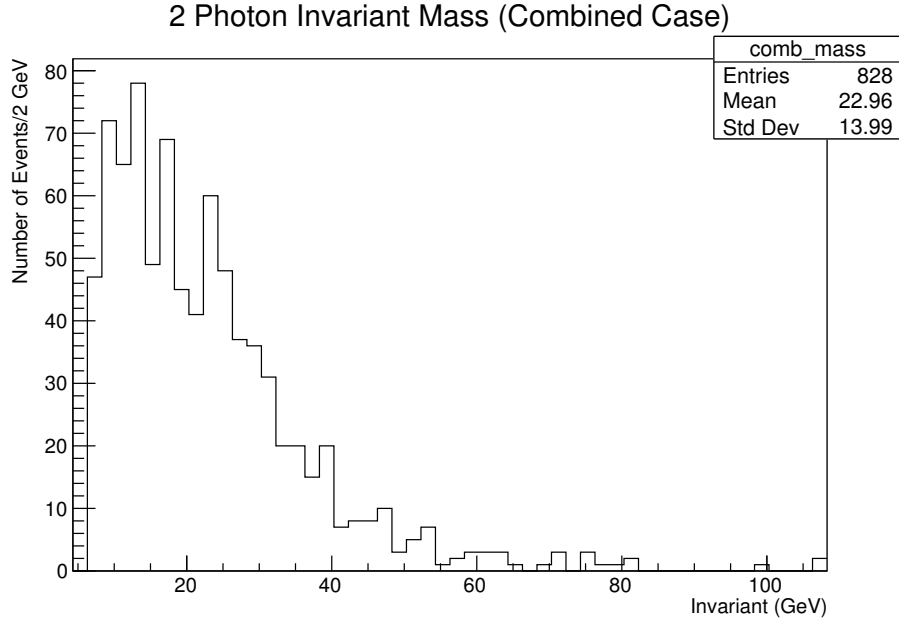


Figure 17: Case 2 Invariant Mass Histogram (Candidate Sample)

According to momentum conservation, the decay photons should recoil opposite of the ISR jet. In Figure 18, the direct recoiling of the trigger decay photon from the ISR jet is shown with a $\Delta R \sim 3.5$ (directly opposite trajectories) is shown.

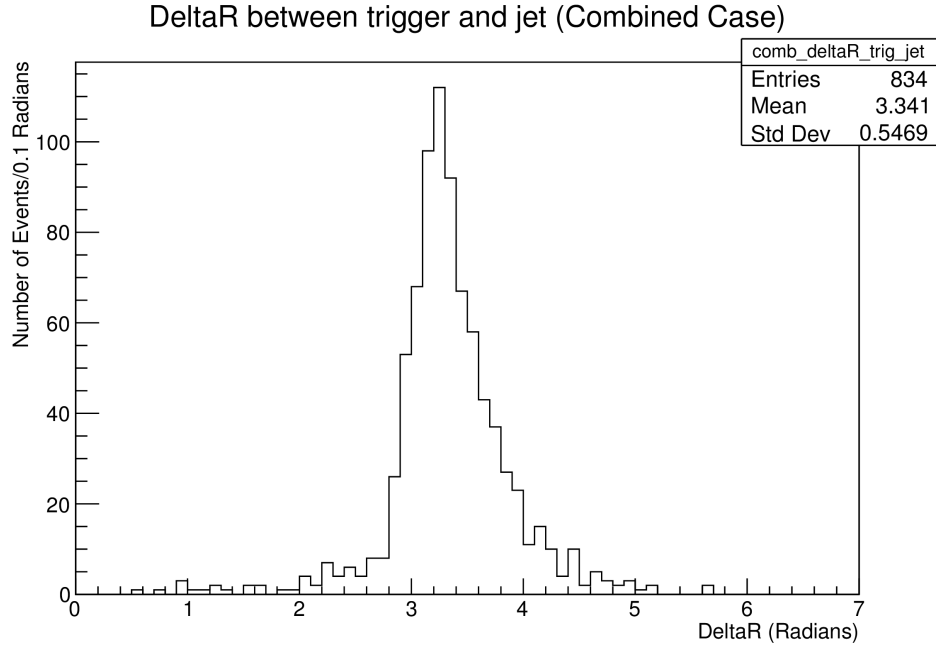


Figure 18: Case 2 ΔR between the trigger photon and the highest energy jet

With the background criteria specified earlier, the mass plot for the control sample is seen in Figure 19.

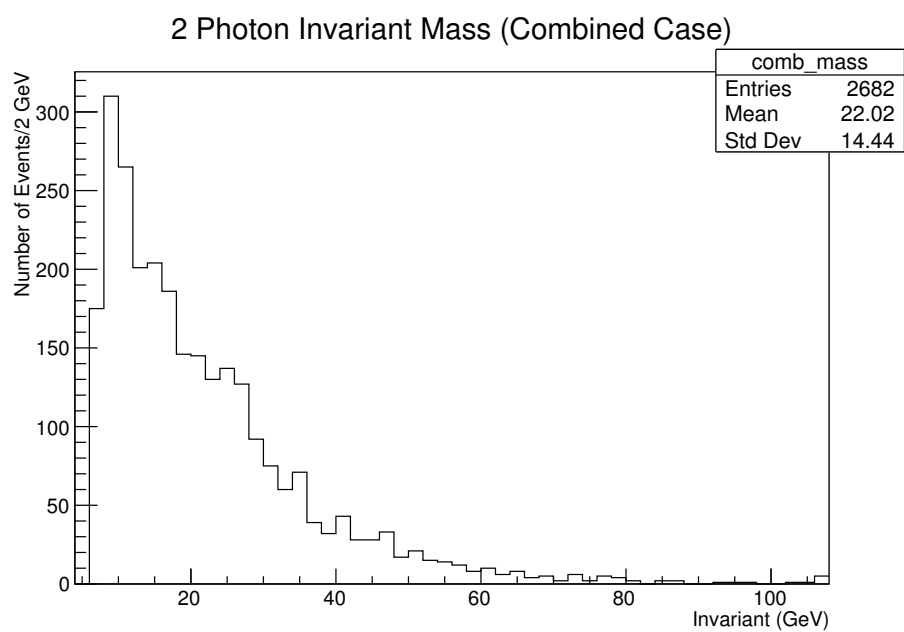


Figure 19: Case 2 Invariant Mass Histogram (control sample)

4 Analysis

Now that the mass plots for the control samples (Figures 14 and 19) and the candidate samples (Figures 11 and 17) have been generated, a statistical analysis must be performed to determine if there is statistically significant evidence for the production of ALPs.

4.1 Background Fit

Using the control sample plots in Figures 14 and 19, and the fitting algorithms in ROOT, a functional form for each histogram can be determined. For both cases a function of the form seen in Equation 7 was used.

$$A * e^{b*x+c*x^2} \quad (7)$$

Where:

A = Amplitude of function

b = Exponential One

c = Exponential Two

The fit for Case 1 control sample is seen in Figure 20. The log scale fit for Case 1 control sample is seen in Figure 21. In Figure 22, the difference between the fit and actual value divided by the uncertainty is shown, this is known as the residual.

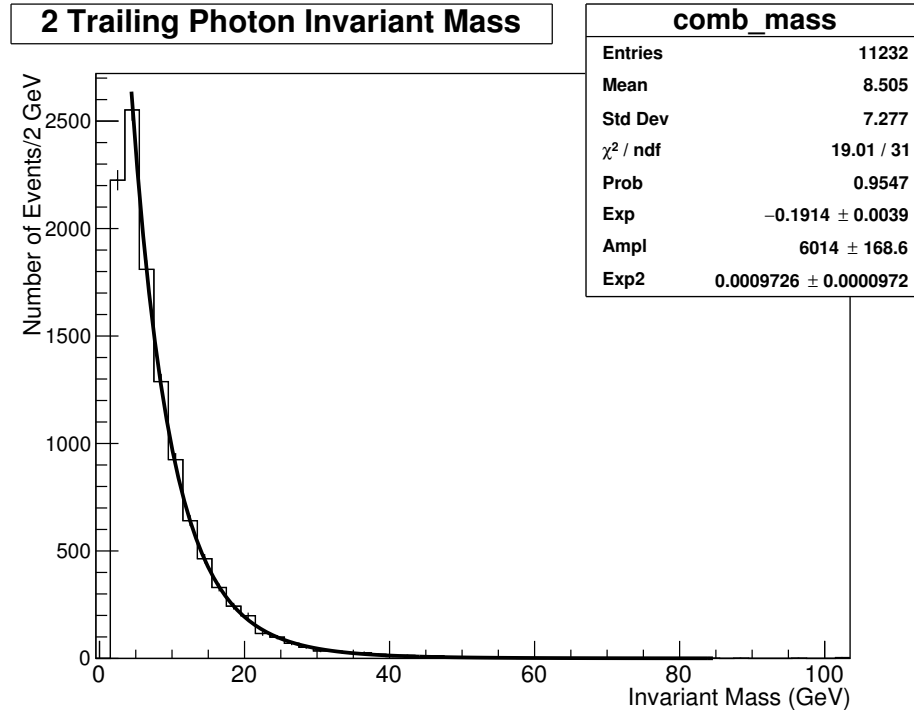


Figure 20: Functional fit of case 1 control sample

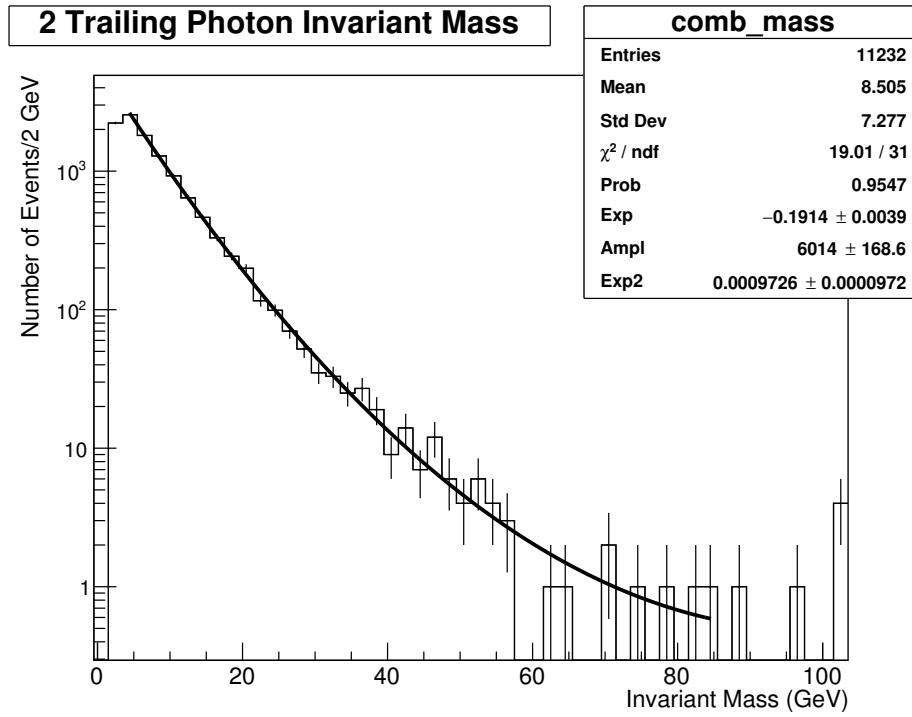


Figure 21: Functional fit of case 1 control sample in log scale y-axis

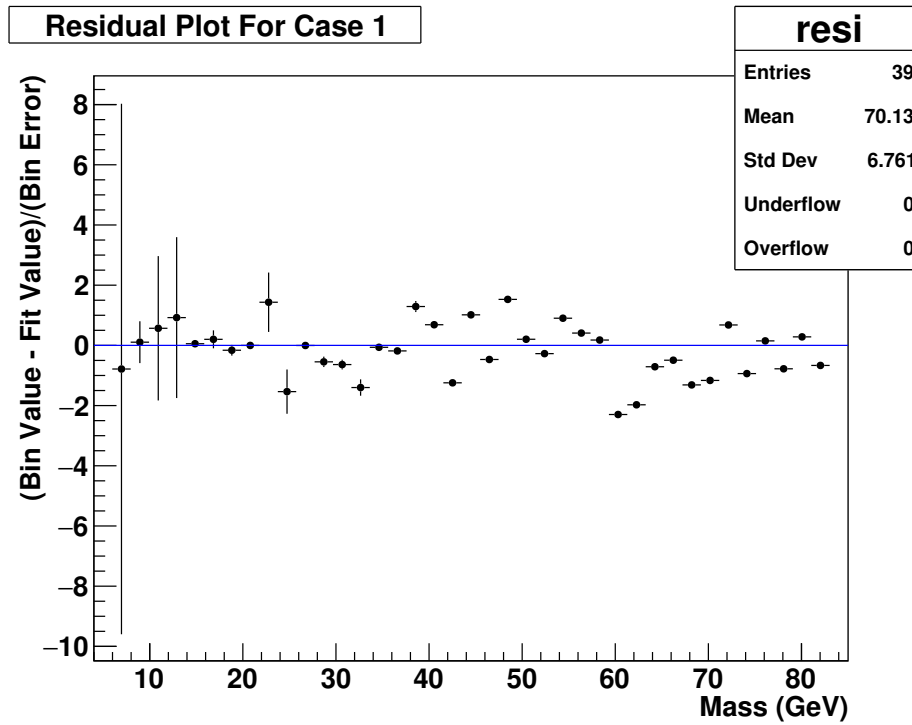


Figure 22: Residuals for fit of case 1 control sample

The fit for Case 2 control sample is seen in Figure 23. The log scale fit for Case 2 control sample is seen in Figure 24. In Figure 25, the difference between the fit and actual value divided by the uncertainty is shown, this is known as the residual.

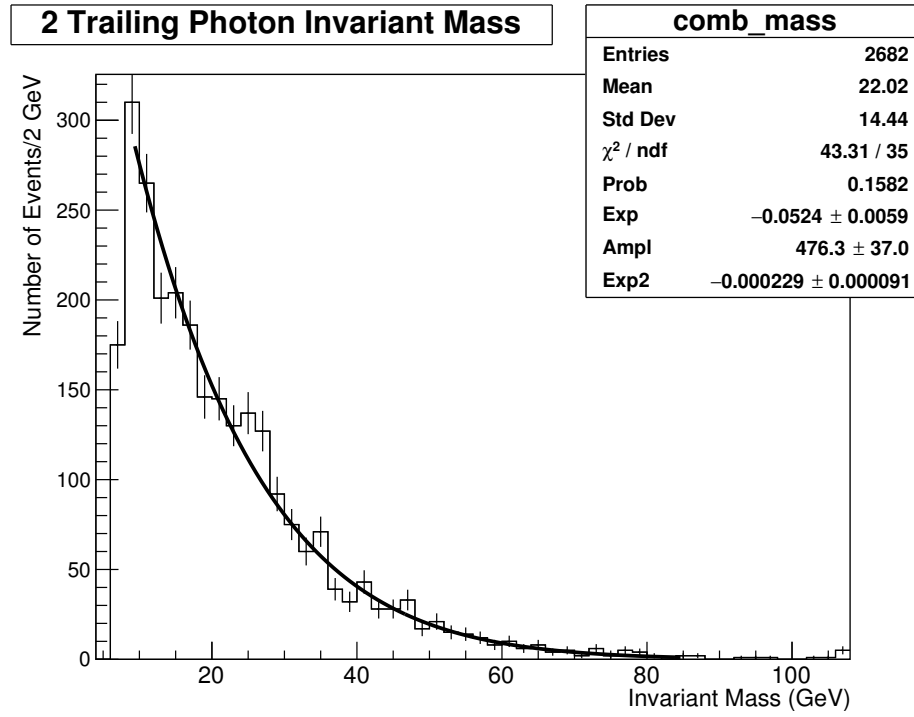


Figure 23: Functional fit of case 2 control sample

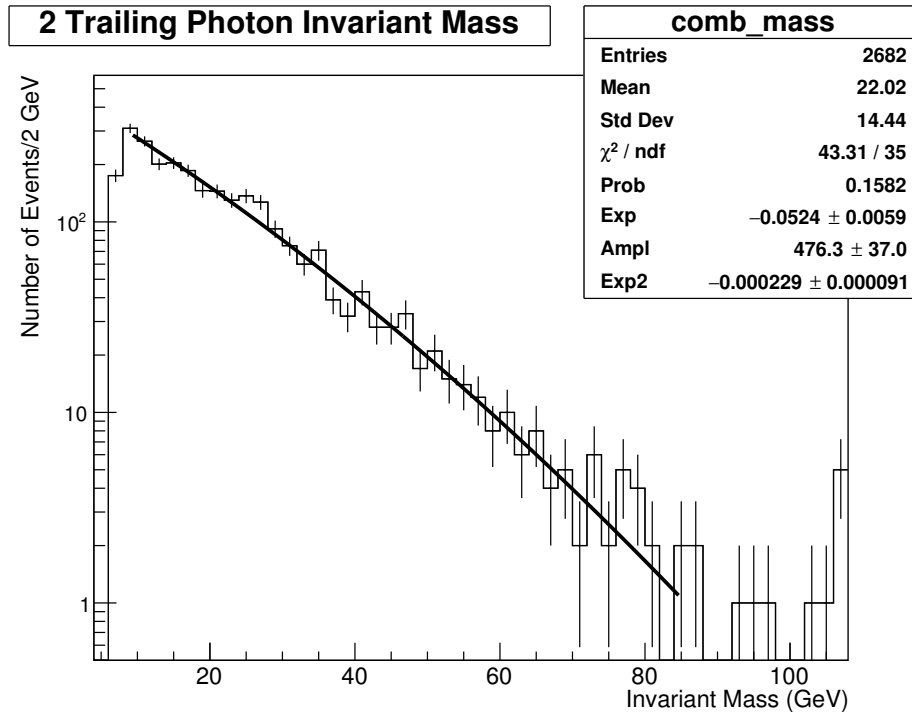


Figure 24: Functional fit of case 2 control sample in log scale y-axis

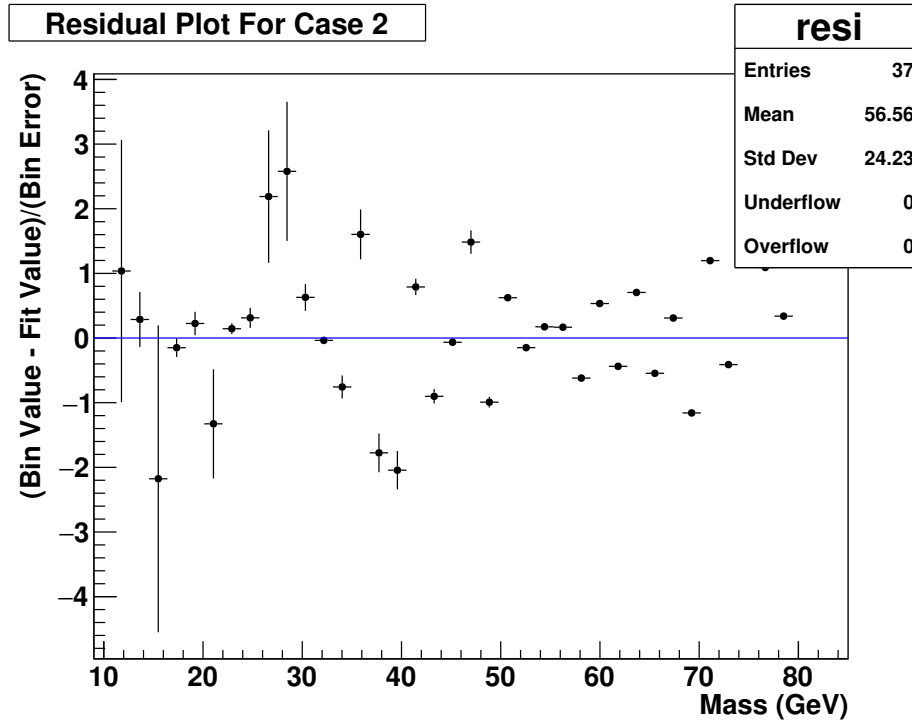


Figure 25: Residuals for fit of case 2 control sample

For the control sample fits of both Case 1 and Case 2, the fit found is reasonable. The probability of fit for the Case 1 fit is 0.9547, and the probability of fit for the Case 2 fit is 0.1582. Even this lower probability for Case 2 is fine when the residuals for both cases are examined (Figures 22 and 25) showing that the fit deviates only slightly in both directions with no obvious bias in the fit.

4.2 Signal Fit

Using the mass plots for candidate samples in Figures 11 and 17. The fit functions found from the control sample can be tested to determine whether the candidate sample plots can be generated from the same functional form.

For the Case 1 candidate sample, the functional form was fitted to the signal with the amplitude allowed to float, and the exponential values fixed within one sigma of the values found in the control sample fit (within the plus-or-minus values next to them). The result is seen in Figure 26. Next the same fit was performed in the same manner but with a Gaussian function added on with specified width (2 GeV) and floating amplitude and mean, The full equation for this fit is seen in Equation 8. The result is seen in Figure 27.

$$A * e^{b*x+c*x^2} + d * e^{-.125*(x-f)^2} \quad (8)$$

Where:

A = Amplitude of function

b = Exponential One

c = Exponential Two

d = Gaussian Amplitude

f = Gaussian Mean

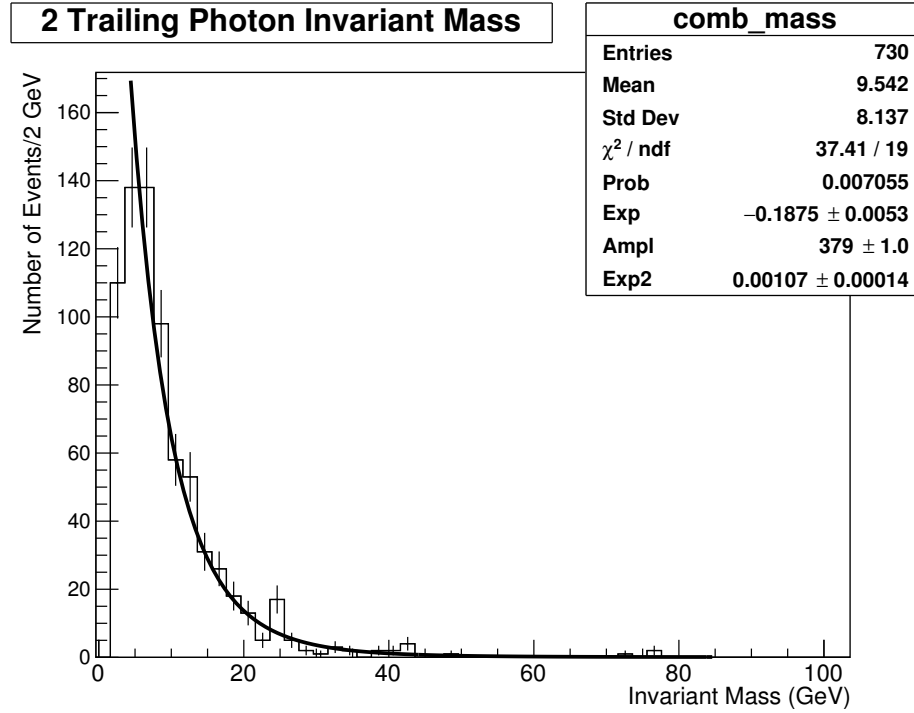


Figure 26: Background functional form fit to candidate sample for Case 1

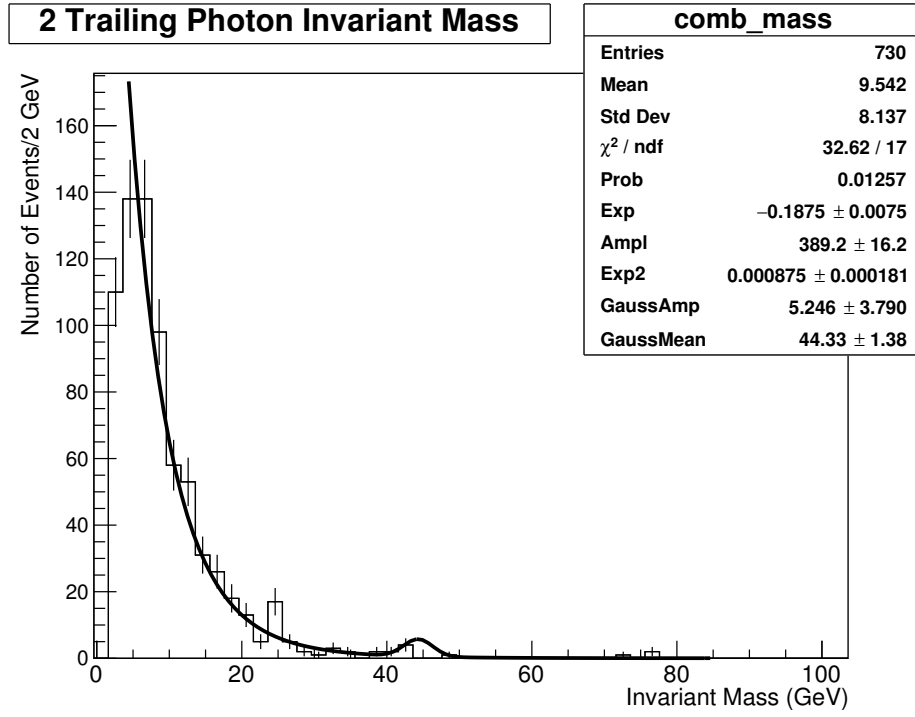


Figure 27: Background functional form plus Gaussian, fit to candidate sample for Case 1

For the Case 2 candidate sample, the functional form was fitted to the signal with all parameters allowed to float. The result is seen in Figure 28. Next the same fit was performed in the same manner but with a Gaussian function added on with specified width (2 GeV) and floating amplitude and mean, The full equation for this fit is seen in Equation 8. The result is seen in Figure 29.

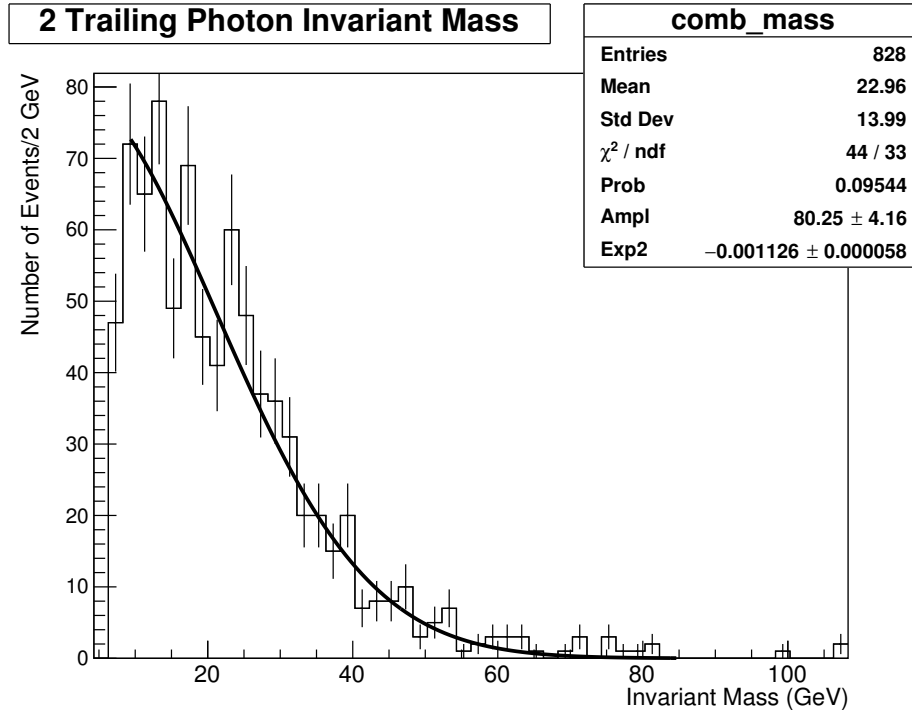


Figure 28: Background functional form fit to candidate sample for Case 2

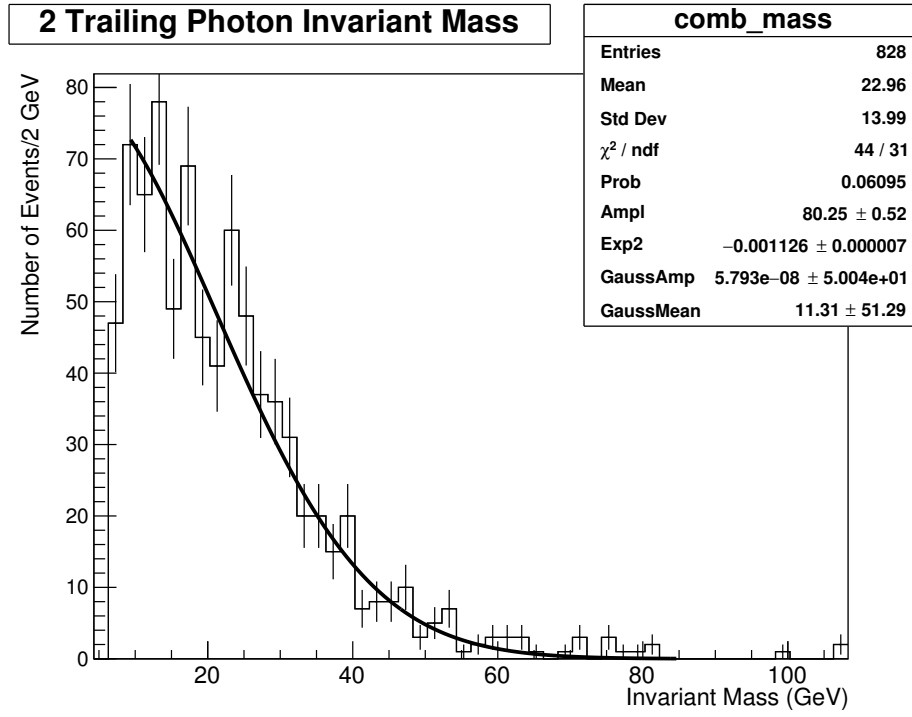


Figure 29: Background functional form plus Gaussian, fit to candidate sample for Case 2

Next the functional form plus Gaussian was fit to the candidate sample with fixed width (2 GeV) and mean, with floating amplitude. The signal strength (amplitude/amplitude uncertainty) was then plotted as a function of gaussian mean. The results for case 1 are seen in Figure 30 and the results for case 2 are seen in Figure 31.

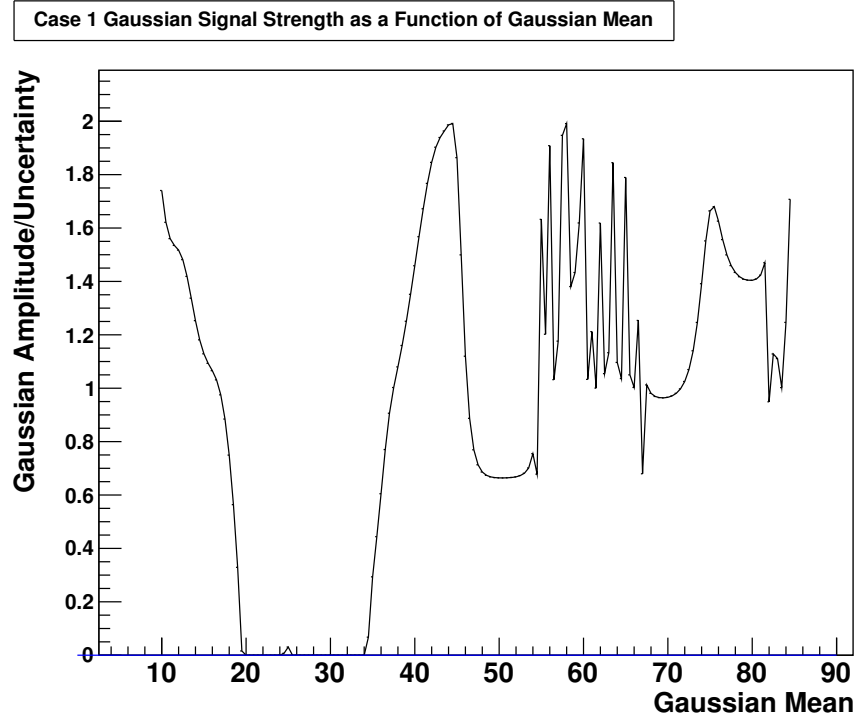


Figure 30: Signal strength as a function of gaussian mean for case 1 candidate sample fit function plus Gaussian fit.

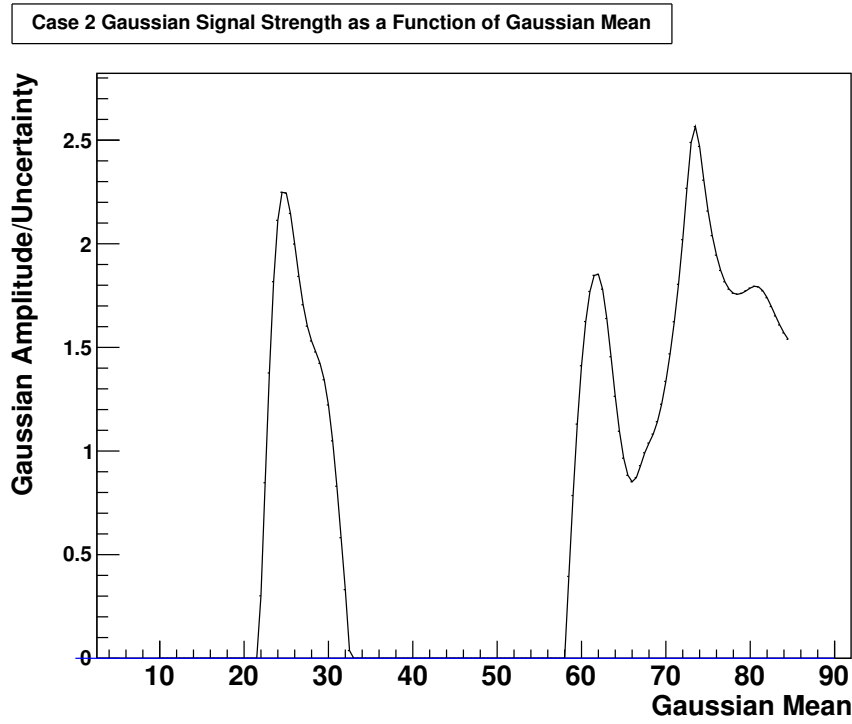


Figure 31: Signal strength as a function of gaussian mean for case 2 candidate sample fit function plus Gaussian fit.

4.3 Hypothesis Testing

The type of analysis being performed is a frequentist analysis, so the probability that the observed signal strength in the candidate samples is a statistical fluctuation, and not a real signal needs to be determined (this is the background only hypothesis). To determine if any excesses observed are more than a simple statistical fluctuation, the signal strengths of random fluctuations is observed. From the converged fits for Case 1 and Case 2 control sample in Figures 20 and 23, 1000 pseudo data histograms are created according to the statistics of the candidate sample histograms (730 events for Case 1, 828 events for Case 2).

These pseudo data histograms then have the fits applied to them in the same manner the candidate sample plots did in Section 4.2 with Figures 26 and 28. The parameters the fits converged to were then plotted.

The Case 1 pseudo data fits parameters and probability of fit are plotted in Figures 32, 33, 34, and 35. The exponential plus gaussian fit converged to

- Amplitude = 389.2
- Exponential = -0.1875
- Exponential2 = 0.000875
- Probability = 0.01257

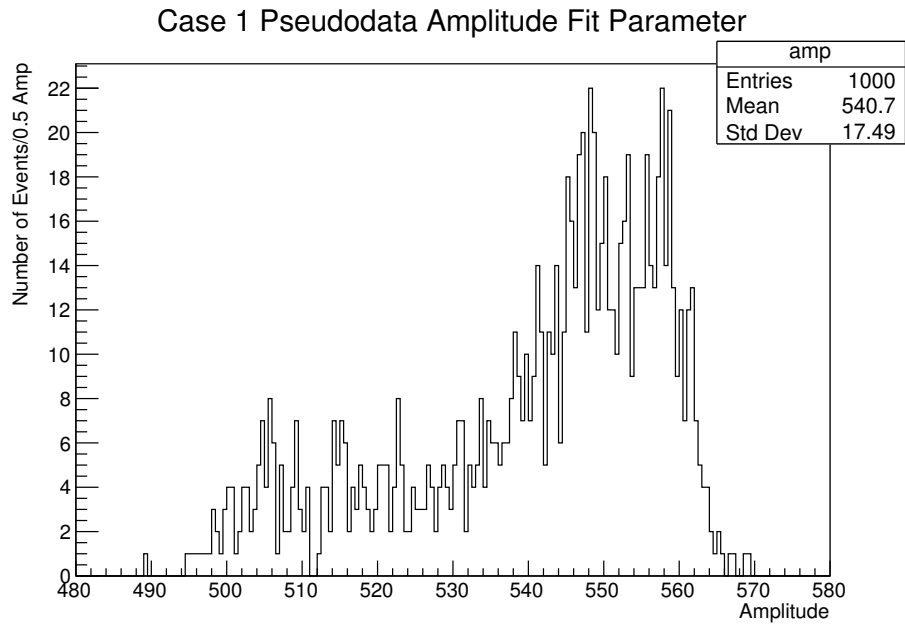


Figure 32: Case 1 pseudo data fits amplitude parameter plot

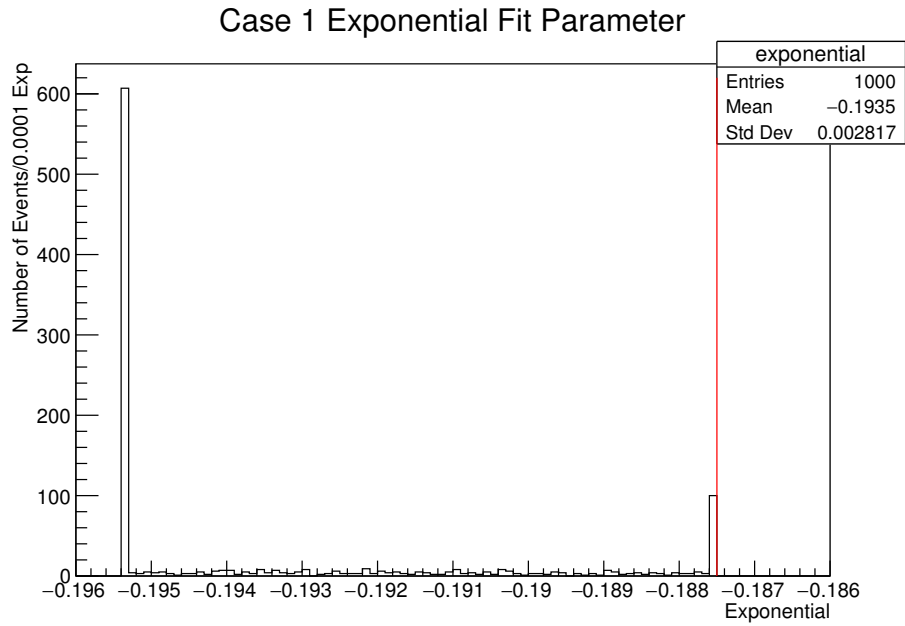


Figure 33: Case 1 pseudo data fits exponential parameter plot. Red line is candidate sample gaussian fit parameter value.

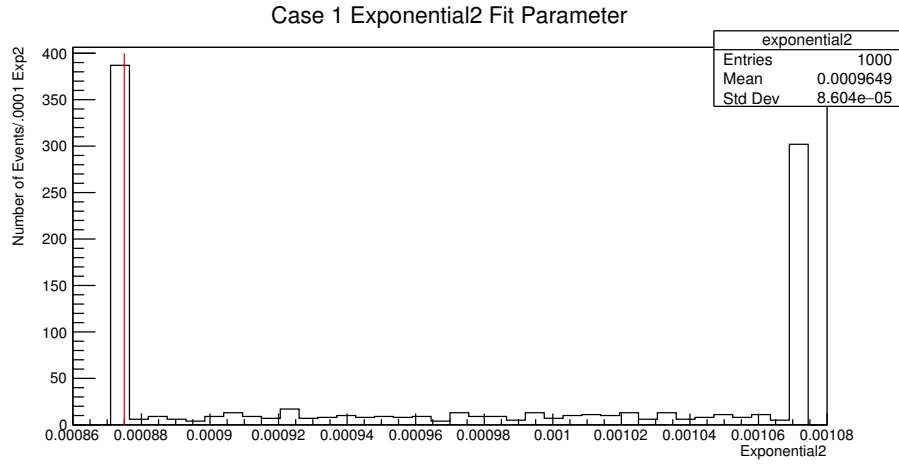


Figure 34: Case 1 pseudo data fits exponential2 parameter plot. Red line candidate sample gaussian fit parameter value.

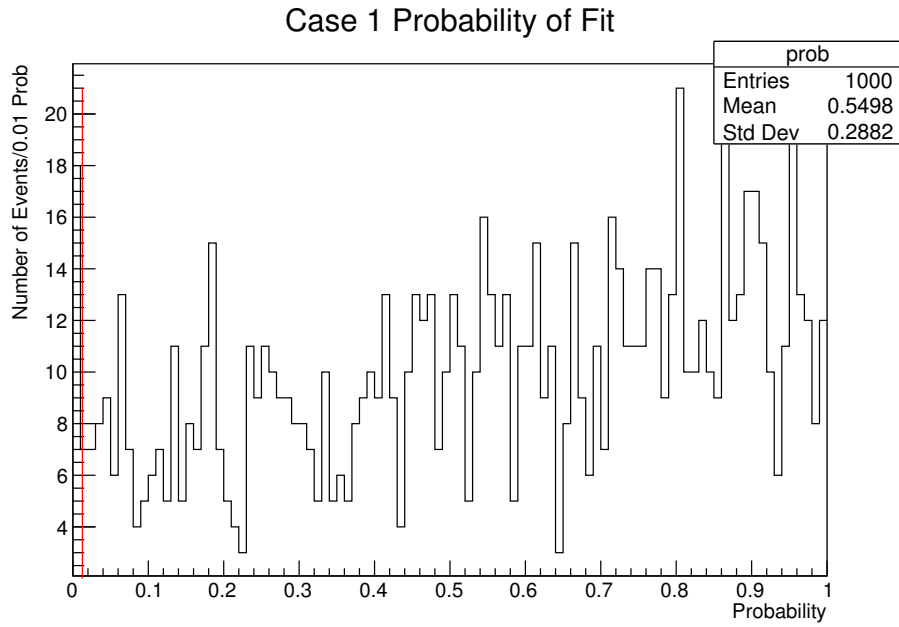


Figure 35: Case 1 pseudo data fits probability of fit. Red line is candidate sample gaussian fit parameter value.

The Case 2 pseudo data fits parameters and probability of fit are plotted in Figures 36, 37, and 38. The exponential plus gaussian fit converged to

- Amplitude = 80.25
- Exponential2 = -.001126
- Probability = .09544

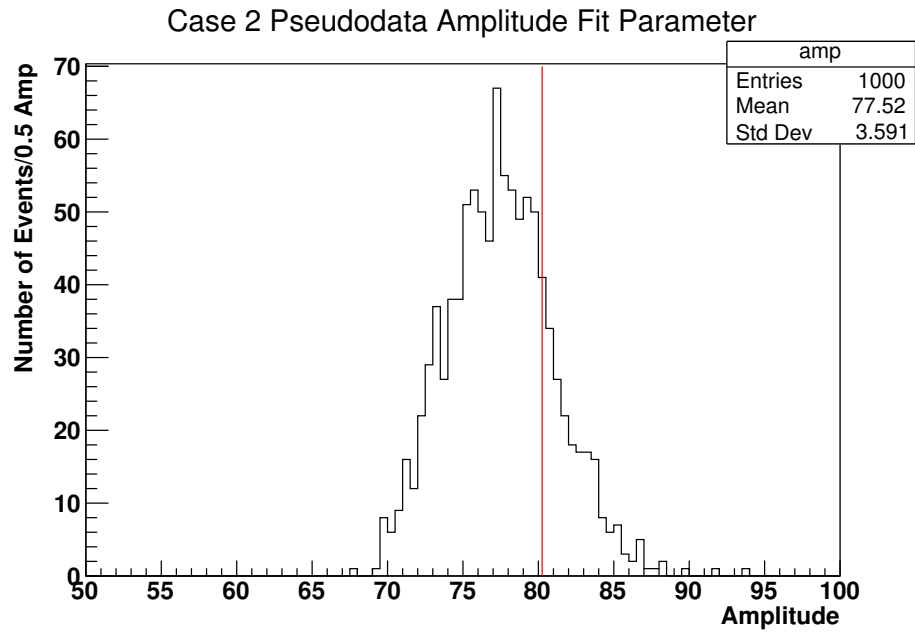


Figure 36: Case 2 pseudo data fits amplitude parameter plot. Red line is candidate sample gaussian fit parameter value.

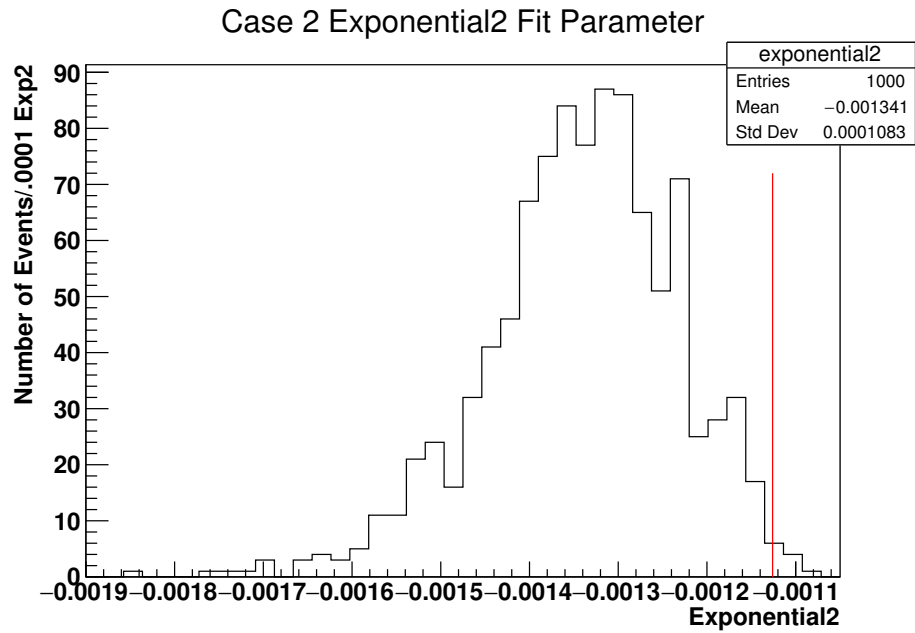


Figure 37: Case 2 pseudo data fits exponential2 parameter plot. Red line is candidate sample gaussian fit parameter value.

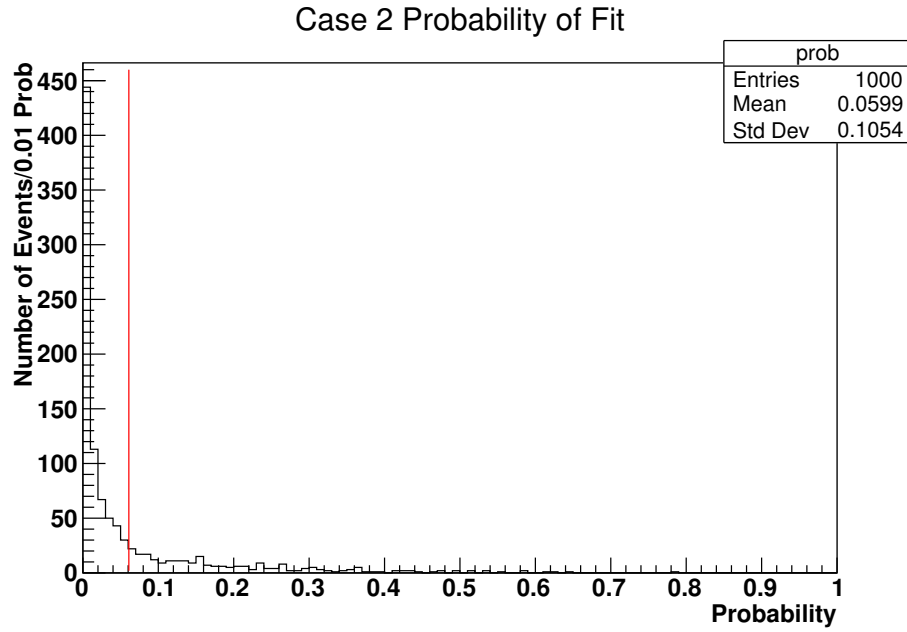


Figure 38: Case 2 pseudo data fits probability of fit. Red line is candidate sample gaussian fit parameter value.

Next each of the pseudo data plots had the exponential plus gaussian fit applied to them, and similarly to what was done in section 4.2 with Figures 30 and 31 the signal strength was plotted as a function of gaussian mean. From these plots, the greatest signal strength was taken and plotted for Case 1 and Case 2 in Figures 39 and 40. The maximum signal strengths for the candidate sample exponential plus gaussian fits were

- Case 1 Maximum Signal Strength = 1.99156
- Case 2 Maximum Signal Strength = 2.56548

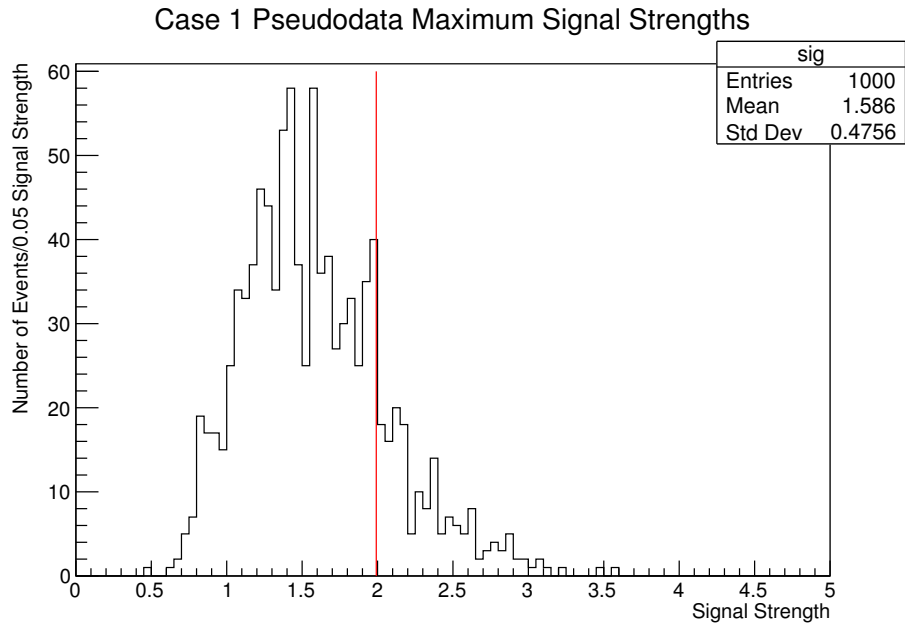


Figure 39: Case 1 pseudo data maximum signal strengths. Red line is candidate sample gaussian fit parameter value.

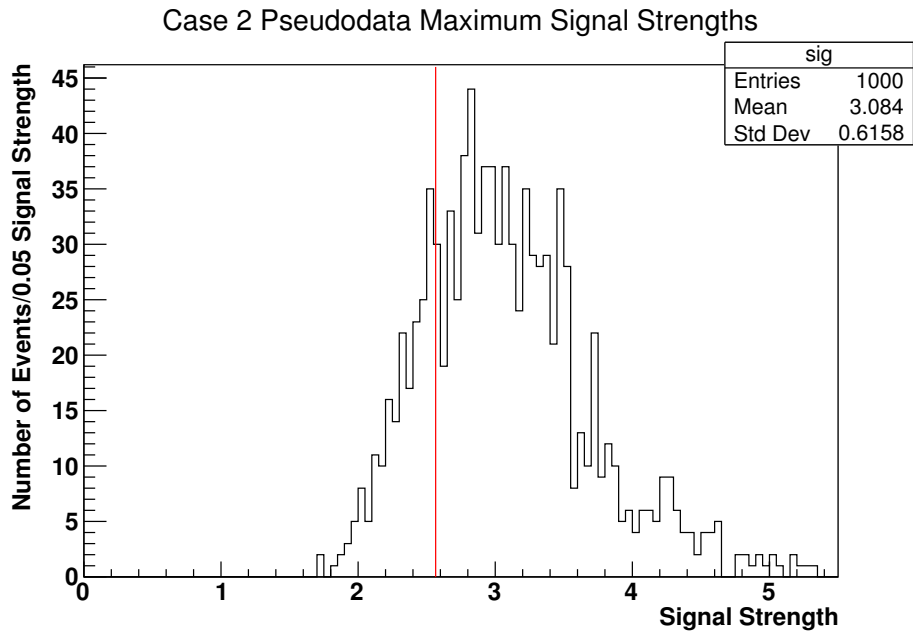


Figure 40: Case 2 pseudo data maximum signal strengths. Red line is candidate sample gaussian fit parameter value.

Using Figures 39 and 40, the p-values for case 1 and case 2 candidate sample gaussian fits can be determined. The p-value is defined as the probability that in the case of the background only hypothesis, a signal strength equal to or greater than the signal strength observed in the candidate

sample is found. This value is calculated by comparing the maximum signal strength in the candidate sample plot (Figures 30 and 31) in each case to the maximum signal strengths from the pseudodata (Figures 39 and 40), and counting the number of times the pseudo data maximum signal strength was greater than or equal to the candidate sample maximum signal strength. This value is then divided by the number of pseudodata experiments (1000 in this thesis), giving the probability that the observed signal strength was greater than or equal to the signal strength from randomly generated data based on the control sample, this is the p-value. In this experiment the p-values were:

- Case 1 p-value: 0.18
- Case 2 p-value: 0.792

5 Conclusions

This thesis searched for the production of axion-like-particles decaying to two high E_T photons with initial state radiation in the low mass region (5 to 85 GeV) using 2018 CMS data at $\sqrt{s} = 13$ TeV. Two cases were examined, the first had an ISR photon for a three photon final state based on a 54.67 fb^{-1} luminosity sample. The second had an ISR jet for a two photon plus jet final state based on a 59.96 fb^{-1} luminosity sample. In both cases no statistically significant excess was observed in the region being examined. Future searches of this type will likely need a greater luminosity, so that more candidate events can be examined to search for the production of axion-like-particles.

References

- [1] Wu, D. (1991, September). “A Brief Introduction to the Strong CP Problem”. *Z.Naturforsch.* A52 (1997) 179-181. <http://inspirehep.net/record/319885/>
- [2] Irastorza, I. G., and Redondo, J. (2018, January 24). “New experimental approaches in the search for axion-like particles”. *Prog.Part.Nucl.Phys.* 102 (2018) 89-159. <https://inspirehep.net/record/1650185>.
- [3] A. Mariotti, D. Redigolo, F. Sala and K. Tobioka, “New LHC bound on low-mass diphoton resonances” *Phys. Lett. B* **783**, 13 (2018).
- [4] http://www.hep.fsu.edu/~askew/wbpge/Askew_PhotonHATS_Width.pdf
- [5] V. Khachatryan *et al.* [CMS Collaboration], “Search for diphoton resonances in the mass range from 150 to 850 GeV in pp collisions at $\sqrt{s} = 8$ TeV,”. *Phys. Lett. B* **750**, 494 (2015)
- [6] <http://cms.web.cern.ch/news/detector-overview>
- [7] <http://cms.cern/detector>
- [8] https://en.wikipedia.org/wiki/Particle_shower
- [9] <https://twiki.cern.ch/twiki/bin/view/CMSPublic/SWGuideEcalRecoClustering#IslandD>